Hybrid Focusing Metric for Sound Speed Estimation in Photoacoustic Imaging Involving Layered Media

Ahmet Yıldırım
Istanbul Technical University
Aslı Nur Mahmutoğlu
Istanbul Technical University
Berkay Karaaslan
Istanbul Technical University
Özgür Özdemir (ozdemiroz3@itu.edu.tr)
Istanbul Technical University

Research Article

Keywords: Photoacoustic Imaging, Focusing Function, Autofocusing, Speed of Sound Estimation, Layered Medium

Posted Date: July 27th, 2022

DOI: https://doi.org/10.21203/rs.3.rs-1626879/v2

Hybrid Focusing Metric for Sound Speed Estimation in Photoacoustic Imaging Involving Layered Media

Ahmet Yıldırım, Aslı Nur Mahmutoğlu, Berkay Karaaslan and Özgür Özdemir

Electronics and Communication, Istanbul Technical University, Street, Istanbul, 34467, Turkey.

Contributing authors: yildirima16@itu.edu.tr; mahmutoglu16@itu.edu.tr; karaaslanb16@itu.edu.tr; ozdemiroz3@itu.edu.tr;

Abstract

In photoacoustic imaging, the speed of sound distribution (SoS) of background is required for image reconstruction, though, in general, it may not be known exactly before reconstruction. The estimation of SoS in a layered media is a difficult task due to the nonlinearity of the wave propagation. In this work, we proposed a novel hybrid focusing metric for accurate image quality assessment in an autofocusing approach to estimate the speed of sound distribution of layered media. In the proposed metric, contrast resolution and spatial resolution information were combined into a novel hybrid focusing metric by exploiting intensity-based focusing metrics and pixel count metrics, thus, enhancing the accuracy of estimation. We have compared the performance of the proposed metric with state of art focusing metrics Brenner, Tennenbaum, and Normalized Variance through numerical simulations which were conducted through k-Wave toolbox. and proved that the proposed focusing metric improved the performance of autofocusing approach significantly in layered media.

Keywords: Photoacoustic Imaging, Focusing Function, Autofocusing, Speed of Sound Estimation, Layered Medium.

1 Introduction

Photoacoustic imaging (PAI) is a novel hybrid imaging modality combining optics and ultrasound techniques and is considered as a very promising complementary diagnostic technique for cancer diagnosis [1–3]. PAI is based on the principle of the heating of tissue with non-ionized optical stimulation which causes an expansion-contraction movement and as a result, tissue acts as an acoustic wave source. The measured acoustics signals by ultrasonic transducers are converted into a photoacoustics image by one of the reconstruction algorithms [4–8]. Among these imaging algorithms, the Time Reversal algorithm has been popular due to its flexibility in the dependence of medium characteristics [5, 6].

Most of the time, the speed of sound (SoS) distribution of the background medium where the target is located is not known and in reconstruction, it is assumed to be some known value. The false assumption of the SoS distribution causes a degradation in the image quality, especially in layered media due to the nonlinearity of the wave propagation. False assumption of the SoS distribution might cause serious consequences. For example, a mistake in SoS of skin tissue which is composed of three layers of epidermis, dermis, and hypodermis, [9] might cause an inaccurate assessment of the cancer lesion. Therefore, SoS distribution should be estimated before or simultaneously with reconstruction.

To address this problem, several sound speed estimation methods have been developed for photoacoustics imaging [10–16]. In [10, 11], an autofocus approach was adopted to photoacoustic imaging to determine the sound speed automatically in a homogeneous medium. Autofocusing approach uses a focus measure which is varied by one of the system parameters to focus automatically on the sharpest or focused image [17–19]. In [10], the sound speed was chosen as a system parameter and a set of photoacoustic images was reconstructed. The speed of sound was then determined by maximizing the focusing metrics of Brenner Gradient, Tenenbaum Gradient, and Normalized Variance which are functions of image contrast. In another autofocusing approach[11], a coherence factor value of received radio-frequency (RF) channel data was used as a focusing measure to choose the focused image and speed of sound. Both autofocus approaches have been validated in homogeneous medium and to the best of our knowledge, there has not been any autofocus method developed for layered media.

For SoS estimation in layered media, a cross-correlation with received RF channel data from a two concentric ring-shaped transducer array was utilized in [12]. There are also several joint reconstruction approaches that have been developed to estimate both the speed of sound and initial pressure simultaneously in inhomogeneous media [13–16]. In [13], a joint reconstruction problem has been formulated as an optimization problem in which the parameterized SOS distribution was simultaneously estimated with absorbed optical energy density. The objective function was defined in terms of data and then solved by alternating the full-wave iterative method. In [15], an iterative nonlinear joint reconstruction algorithm without constant speed assumption was developed based on the finite element solution of the photoacoustic wave equation.

In this work, we have developed a novel focusing metric for autofocusing approach to estimate the speed of sound distribution in layered media for photoacoustics imaging. Our motivation was to extend the previous autofocusing approach developed for homogeneous medium to the layered structure of skin tissue. It is known that wave propagation in layered media is subject to multiple reflections which dramatically increases the complexity of the relation between the image quality and the sound speed distribution. Thus the assessment of the image quality with only image contrast can no longer provide enough accuracy in layered media. To assess the image quality accurately, we have proposed to use spatial resolution information in conjunction with image contrast (contrast resolution) in the focusing metric. To this end, we have defined a novel focusing metric Hybrid Focusing Metric(HFM) as a combination of intensity-based metrics such as Brenner and Tenenbaum gradient functions and Thresholded Pixel Count (TPC) metric which gives the support of the image feature [17, 18]. In the proposed approach, a focused image was defined as the one having the maximum intensity sharpness with the smallest support. Since the focused image should be chosen automatically, we have combined Otsu's thresholding method into the TPC function to choose the thresholding value in TPC automatically. The enhancement in the accuracy of SoS estimation in layered media by the proposed HFM was demonstrated by comparing it with existing focusing functions through the numerical simulations with k-wave toolbox [20].

2 Methodolodgy

In photoacoustics imaging, a laser pulse is used for optical stimulation of the tissues which causes an expansion-contraction movement and creates an initial acoustical pressure field, p_0, see Fig. 1. The initial acoustical pressure field propagates through the tissue and measured by transducer array on the surface. The relationship between the measured acoustical pressure $p(\vec{r},t)$ and the initial pressure distribution can be given as following photoacoustics wave equation[2] :

$$\nabla^2 p(\mathbf{r},t) - \frac{1}{c(r)^2}\frac{\partial^2}{\partial t^2}p(\mathbf{r},t) = \frac{-\beta}{C_p}p_0(\mathbf{r})U(t) \quad (1)$$

where $c(\mathbf{r})$ is the sound speed distribution of the medium, β is the thermal expansion coefficient, C_p is the specific heating capacity. $p_0(\mathbf{r})$ is initial pressure distribution and $U(t)$ is the temporal profile of laser pulse. The PAI imaging

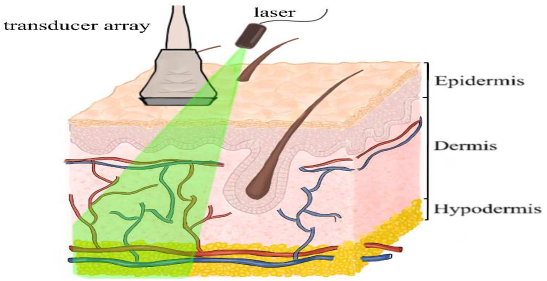

Fig. 1: Schematic Photoacoustic Imaging Set-up for Skin

algorithms reconstruct the initial pressure distribution $p_0(\mathbf{r})$ from the measured pressure on the surface with an ultrasound probe. In this work, we have used Time reversal algorithm as a reconstruction algorithm which refocuses the measured acoustic field to the reconstruction region to image the initial pressure source, [5, 6]. It is important to note that photoacoustic tomographic imaging belongs to the inverse source problems which are typically ill-posed problems where the solution is highly sensitive to error in data [21]. Thus, a false assumption of sound speed distribution of the medium causes a severe distortion in the reconstructed image.

2.1 Focusing Metrics and Image Quality

Focusing metrics (sharpness functions) that assess image quality can be classified into two main categories: focusing functions based on image contrast (intensity-based) and focusing functions based on a number of pixels above a given threshold [17, 18]. Three of the intensity-based focusing functions, gradient-based Brenner and Tenenbaum function, and statistical-based Normalized Variance function have been applied to quantify the sharpness of photoacoustics image in a homogeneous medium successfully in [10].

Let $I(x, y)$ be the intensity of the reconstructed photoacoustics image. *Brenner* function computes the summation of the square of the first-order difference of image intensity between a pixel and its neighbor with a distance of two:

$$\begin{aligned} F_{Br} = \sum_{x,y} \left[I(x+2,y) - I(x,y)\right]^2 + \\ \left[I(x,y+2) - I(x,y)\right]^2 \end{aligned} \tag{2}$$

Tenenbaum computes the summation of gradient vector components of the image which is convolved with Sobel operators g:

$$F_{Tn} = \sum_{x,y} \left[\mathbf{g} * I(x,y)\right]^2 + \left[\mathbf{g}^\intercal * I(x,y)\right]^2, \tag{3}$$

Normalized Variance function is based on the statistical distribution of image intensity and calculates the variations in the pixel values about the mean intensity μ:

$$F_{NV} = \frac{1}{\mu} \sum_{x,y} \left[I(x,y) - \mu\right]^2 \tag{4}$$

The sharpness value obtained by these focusing functions is only determined by the image intensity value and the support information (number of pixels) of the image features is not taken into account. This implies that the image sharpness is defined only in terms of contrast resolution and not in terms of spatial resolution. These metrics give a very good result of estimation in a homogeneous medium, though, their accuracy deteriorates considerably in a layered medium in which a small deviation from a true speed of sound values causes considerable distortion in the reconstructed image, such as spreading the support of image of photoacoustic source. This is mainly due to the nonlinearity of wave propagation with multiple reflection effect in a layered medium. The spread image means a large number of pixels which might cause a false sharpness maximum value in intensity-based metrics which sum the pixel intensities or intensity differences.

Second class of focusing metrics, thresholded-based focusing function Thresholded Pixel Count (TPC) determines the sharpness value as the number of pixels above threshold value which corresponds to the support of the image feature. In TPC, the image is first converted into a binary image by using a specified threshold value, τ as follows:

$$f(x,y) = \begin{cases} 1, I(x,y) \geqslant \tau \\ 0, I(x,y) < \tau \end{cases} \tag{5}$$

Then the pixel count is achieved by summing the intensity of the binary image:

$$F_{TPC} = \sum_{x,y} f(x,y) \tag{6}$$

Since the number of pixels belonging to the image is considered as the sharpness of the image, one can conclude that TPC calculates the sharpness value from the spatial resolution information of images. The use of TPC in autofocusing in a layered medium may cause false estimation since different SoS combinations can produce images with the same number of pixels due to the ill-posedness of the imaging problem.

2.2 Hybrid Focusing Metric

To address the drawbacks of the aforementioned focusing metrics in layered medium, we propose a novel focusing metric called Hybrid Focusing Metric (HFM) by exploiting both contrast resolution and spatial resolution information simultaneously. Our approach simply searches for the optimum combination of SoS which ensures the maximum intensity sharpness with the smallest support. To this aim, the total intensity sharpness value, $F_{Intensity}$ was normalized with the number of pixels determined by TPC, F_{TPC} as follows:

$$F_{HFM} = \frac{F_{Intensity}}{F_{TPC}} \tag{7}$$

In the proposed approach, the intensity sharpness value $F_{Intensity}$ can be determined by one of the intensity-based focusing functions, Brenner, Tenenbaum, or Normalized variance. For the accuracy of HFM, the determination of the right number of pixels in the image with TPC was very crucial. It should be noted that the critical point of TPC is the choice of threshold value to apply the threshold and convert the intensity image into a binary image. It is also important to choose it automatically for each image since it is used for automatic search in speed estimation. Therefore, we exploited Otsu's Method combined with TPC for the determination of threshold value since it provides threshold value automatically for each image and is suitable for photoacoustics images [22].

Using the proposed HFM, the auto-focusing for the layer speed estimation was achieved as follows: the speed of sound in each layer was varied and the corresponding image was reconstructed by Time Reversal algorithm. Then the sharpness density value of all reconstructed images was determined by the proposed HFM. The sound speed combination maximizing the sharpness value was then chosen as a true SOS and the corresponding image was chosen as a focused image. We have applied an exhaustive search strategy for the search for maximum sharpness value. The flowchart to visualize the steps of the proposed approach is presented in Fig.2.

We should note that the proposed approach is not limited to the intensity-based metrics given above, it can be extended to any other intensity metric in principle.

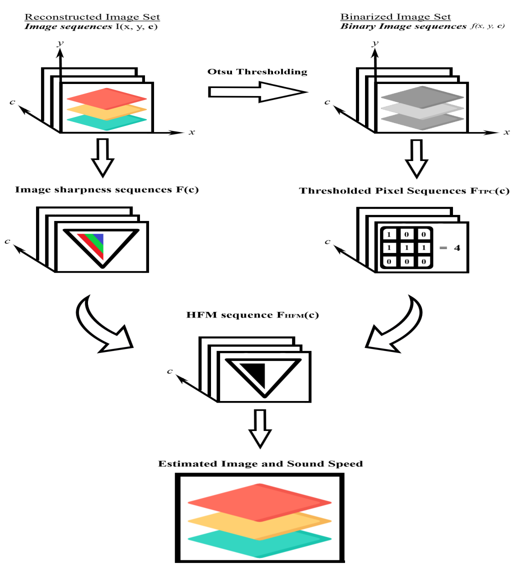

Fig. 2: Flowchart of the sound speed estimation with Hybrid Focusing Method

3 Numerical Results

To evaluate the performance of the proposed method, numerical experiments were conducted through simulations with k-wave toolbox [20]. In all examples, the size of the region of interest

(ROI) was chosen as $3.3mm$ by $3.3mm$ which corresponds to the 133 grid points in each axis where the distance between each grid point in both the x and y-axis is 0.025mm. A linear transducer array with 128 elements was placed along the measurement line of $3.3mm$ length. The center frequency of transducers was set to 24.5MHz. The source of initial pressure was modeled as a point source(with a radius of 0.025mm, grid size). The center frequency was chosen as 24.5MHz.

3.1 Comparison with Existing Methods

We first compared the performance of our method in layered medium with existing metrics. To this aim, two layered medium was considered where the speed of sounds in upper and lower layers are $c_1 = 1600m/s$ and $c_2 = 1500m/s$, respectively, Fig. 3a. Two point sources were placed in the center of each layer.

A) Two-layered medium with one unknown speed:
We first assumed that only upper layer speed, c_1 was unknown and searched for it by varying the speed from $1300m/s$ to $1700m/s$ with $25m/s$ steps and 17 different image were reconstructed. The variation of normalized focus functions versus the sound speed of upper layer, c_1 is given in Fig. 3. Here, We named the proposed metric as HFM Brenner when it was formulated using Brenner function and so on. As seen from Fig. 3, Brenner and Tenenbaum functions had their maximum at 1300 m/s which was a false estimation while the proposed HFM, TPC and Normalized Variance (NV) metrics estimated the true speed of 1600 m/s. Note that the choice of the intensity based focusing functions in HFM was not crucial since all of them provide similar behaviour in estimation. We should also note that the contour curves of HFM have sharper peak than that of TPC and NV which is required for autofocusing function to identify the maximum precisely.

Reconstructed images with estimated SoS values by each function and exact SoS value were presented in Fig. 4. As HFM, TPC and Normalized Variance (NV) function estimated the speed accurately, the reconstructed image using true value was chosedn as a focused image. On the other hand, Brenner and Tenenbaum Gradient metrics calculated the sharpness value of

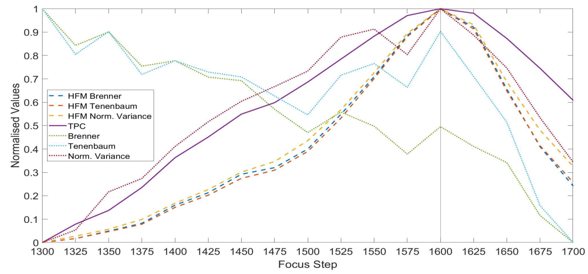

Fig. 3: The variation of the normalized focus functions versus speed of sound c_1

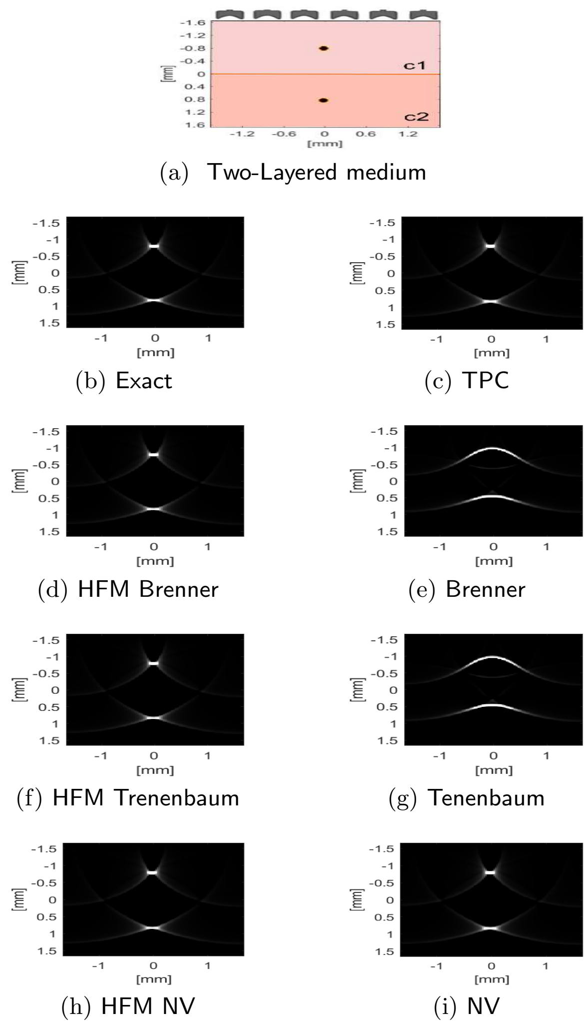

Fig. 4: (a)Considered two-layered medium Reconstructed image with (b) exact SoS distribution (c) TPC (d) HFM with Brenner (e) Brenner (f) HFM with Tenenbaum (g) Tenenbaum (h) HFM with NV (i) NV

the reconstructed image with spreaded support, see Fig. 4e and 4g as a maximum which lead to inaccurate estimation. The reason of this can be explained with the fact that they determined the sharpness as a summation of the intensity differences from all the contributing pixels, thus, their sharpness value became larger in spreaded support than the exact reconstruction.

B) Two-layered medium with two unknown speeds:

As a second case, we considered both layer speed unknown in two-layered medium. The actual speeds of sound in upper and lower layers were $c_1 = 1500m/s$ and $c_2 = 1400m/s$, respectively. In the reconstruction, the speed range between 1300 and 1700 m/s was swept with 25 m/s steps for both layers, thus, 289 different images were reconstructed. The contour plot of the focusing functions in two variables were presented in Fig. 5 It was seen that Brenner and Tenenbaum functions did not have a peak around true speed and therefore, they estimated false SoS, (1300,1700) and (1475,1700), respectively. NV function had one closer peak to the true SOS, though it had several local maximum and gave estimation as (1500,1300). NV function had better estimation, (1500,1300), than the others, yet, the estimation of the second layer was not close to true speed. On the other hand, even though TPC provided more focused contour map than the intensity based metrics, the range of estimation was still quite large and estimated SOS as (1525,1325). The proposed HFM enhanced the estimation of more accurate optimization for true estimation and estimated SOS as (1500, 1375).

3.2 Skin-mimicking three-layered medium

To assess the performance of HFM in photoacoustics imaging of skin which is composed of layers of epidermis, dermis and hypodermis, the SoS distribution estimation in three-layered medium was examined. To mimic skin, the thickness of the layers were chosen accordingly as $0.1mm$, $1.2mm$ and $2mm$, see Fig. 7a. and the layers speeds were set to speed in skin layers as $c_1 = 1625m/s$, $c_2 = 1575$, $c_3 = 1450$ for epidermis, dermis and hypodermis, respectively, [9]. HFM, Brenner function was chosen as an intensity based focusing metric.

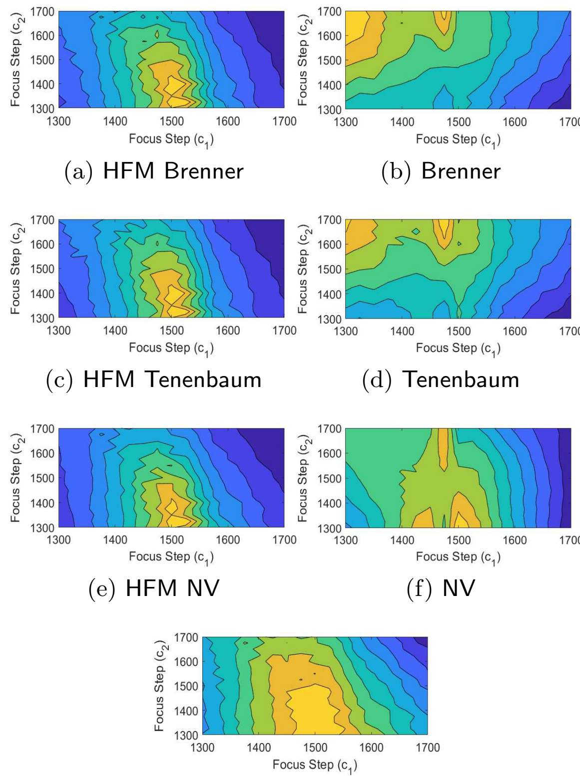

(a) HFM Brenner (b) Brenner (c) HFM Tenenbaum (d) Tenenbaum (e) HFM NV (f) NV (g) TPC

Fig. 5: Contour plot of focusing function (a) HFM Brenner (b) Tenenbaum (c) HFM Tenenbaum (d) Brenner (e) HFM NV (f) NV (g) TPC.

A) Three-layered medium with one unknown speed:

The considered configuration was given in Fig. 7a. The measurement was performed on the top of the first layer epidermis. As a first case, only one of the layers was assumed to be unknown and HFM was applied to estimate it by varying the speed from 1200 to 1800 with a step size of 25. This process was repeated for each layer and in each case, HFM estimated true layer speed, $c_1 = 1625m/s$ for epidermis,$c_2 = 1575$ for dermis and $c_3 = 1450$ for hypodermis.

B) Three-layered medium with two unknown speeds:

In this case, the speed of two layers was assumed to be unknown and HFM was applied to estimate them for all possible combinations of layers. The reconstruction process was performed on 625 different sound speed combinations which correspond to the range of 1200-1800 with 25 steps and

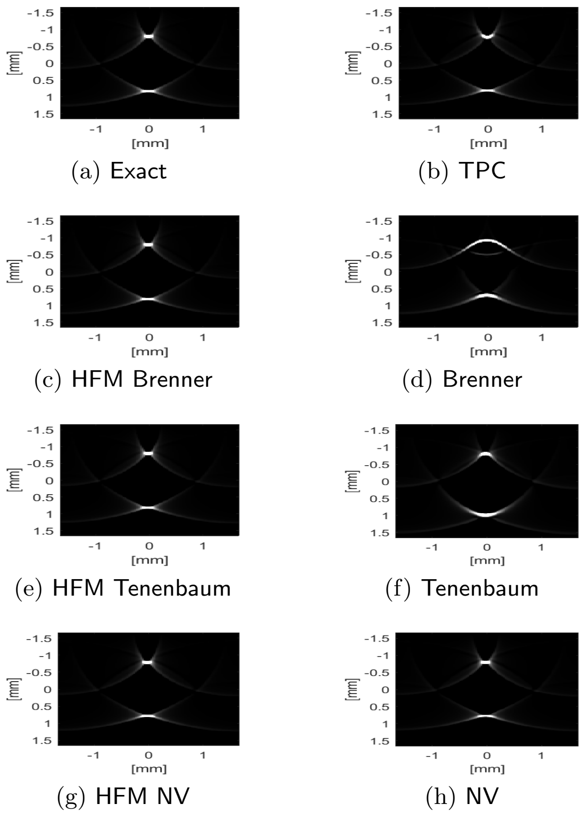

Fig. 6: Reconstructed image with a) exact SOS distribution (b) TPC (c) HFM Brenner (d) Brenner (e) HFM Tenenbaum (f) Tenenbaum (g) HFM NV (h) NV

then the maximum was searched within this set of images. When the sound speed of the epidermis was known, the other two layers' speeds were estimated as $c_2 = 1600m/s$ and $c_3 = 1325m/s$. For the middle layer dermis was known, epidermis and hypodermis were estimated as $c_1 = 1525m/s$ and $c_3 = 1400m/s$. And the final combination, hypodermis was known and epidermis and dermis were estimated as $c_1 = 1450m/s$ and $c_2 = 1600m/s$. It was observed that the estimation of the middle layer, dermis speed was the most accurate and that of the epidermis was the least accurate one within all combinations. These results can be explained by the fact that the epidermis layer was the thinnest layer, too close to transducers which caused more distortion in the quality of the image.

C) Three-layered medium with three unknown speeds:
As a final case, all three layer speed were assumed to be unknown. Simulations were performed within the speed range of 1200-1800 m/sec with a step size of 25, thus, 15625 combinations were examined in total. HFM estimated the layer's speeds as $c_1 = 1450m/s, c_2 = 1600m/s, c_3 = 1300m/s$ and the reconstructed images with exact and estimated speed were depicted in Fig. 7b,c. The speed of dermis was estimated quite accurately, however, the speed of top and bottom layers which were epidermis and hypodermis were not that accurate. The difficulty in epidermis arose from its thickness which was thinnest layer and the source in the epidermis was too close to the transducer array.

To examine the measurement location effect on the estimation, measurement line were changed to top to epidermis layer to bottom of hypodermis layer and speed values were estimated for this setup as $c_1 = 1650m/s, c_2 = 1525m/s, c_3 = 1450m/s$. The estimation of the epidermis and hypodermis were highly improved. The reconstructed images in this case were presented together with the previous reconstruction results in which the measurement were the top of the epidermis layer to have clear comparison in Fig. 7d,e.

4 Conclusion

In this work, we have proposed a novel Hybrid Focusing Metric (HFM) for the use in autofocusing approach to estimate the sound speeds in a layered medium. In the proposed metric, contrast and spatial resolution information were properly taken into account by combining intensity-based metric and pixel counting focusing metric for accurate assessment of the image quality for accurate speed estimation. We have compared the HFM with state of art focusing metrics used in photoacoustics imaging through the numerical simulations for two-layered medium and proved that HFM substantially improved the estimation accuracy. We have examined HFM performance on a skin-mimicking three-layered medium. We should note that the application of the proposed approach is not limited to photoacoustic imaging, it can also be used in ultrasound imaging.

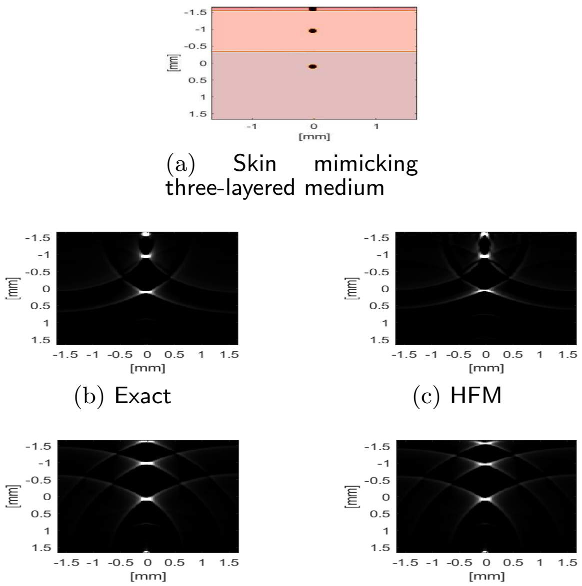

(a) Skin mimicking three-layered medium

(b) Exact (c) HFM

(d) Exact (e) HFM

Fig. 7: (a) Skin mimicking three-layered medium. Reconstructed images: Measurement on the top:(b),(c) Measurement on the bottom: (d),(e)

Data Availability

Data sharing not applicable to this article as no datasets were generated or analysed during the current study.

Funding

This work was supported by TUBITAK under Grant 119E624.

Conflict of Interest

The authors have no relevant financial or non-financial interests to disclose.

References

[1] Xia, J., Yao, J., Wang, L.H.V.: Photoacoustic tomography: Principles and advances. Progress In Electromagnetics Research **147**, 1–22 (2014)

[2] Wang, X., Xu, Y., Xu, M., Yokoo, S., Fry, E.S., Wang, L.V.: Photoacoustic tomography of biological tissues with high cross-section resolution: Reconstruction and experiment. Medical Physics **29**(12), 2799–2805 (2002)

[3] Mehrmohammadi, Y.S.J.Y.D..E.S.Y. M.: Photoacoustic imaging for cancer detection and staging. Current molecular imaging: Ultrasonic Imaging and Tomography **2(1)**, 89–105 (2013)

[4] Xu, M., Wang, L.V.: Universal back-projection algorithm for photoacoustic computed tomography. Phys. Rev. E **71**, 016706 (2005)

[5] Bossy, E., Daoudi, K., Boccara, A.-C., Tanter, M., Aubry, J.-F., Montaldo, G., Fink, M.: Time reversal of photoacoustic waves. Applied Physics Letters **89**(18), 184108 (2006)

[6] Cox, B.t., Treeby, B.e.: Artifact trapping during time reversal photoacoustic imaging for acoustically heterogeneous media. IEEE Transactions on Medical Imaging **29**(2), 387–396 (2010)

[7] Huang, C., Wang, K., Nie, L., Wang, L.V., Anastasio, M.A.: Full-wave iterative image reconstruction in photoacoustic tomography with acoustically inhomogeneous media. IEEE Transactions on Medical Imaging **32**(6), 1097–1110 (2013)

[8] Kim, M., Jeng, G.-S., Pelivanov, I., Odonnell, M.: Deep-learning image reconstruction for real-time photoacoustic system. IEEE Transactions on Medical Imaging **39**(11), 3379–3390 (2020)

[9] Chen, A.I., Balter, M.L., Chen, M.I., Gross, D., Alam, S.K., Maguire, T.J., Yarmush, M.L.: Multilayered tissue mimicking skin and vessel phantoms with tunable mechanical, optical, and acoustic properties. Medical Physics **43**(6Part1), 3117–3131 (2016)

[10] Treeby, B.E., Varslot, T.K., Zhang, E.Z., Laufer, J.G., Beard, P.C.: Automatic sound speed selection in photoacoustic image reconstruction using an autofocus approach. Journal of Biomedical Optics **16**(9), 090501 (2011)

[11] Yoon, C., Kang, J., Han, S., Yoo, Y., Song, T.-K., Chang, J.H.: Enhancement of photoacoustic image quality by sound speed correction: ex vivo evaluation. Optics Express **20**(3), 3082 (2012)

[12] Kolkman, R.G., Steenbergen, W., Leeuwen, T.G.V.: Reflection mode photoacoustic measurement of speed of sound. Optics Express **15**(6), 3291 (2007)

[13] Matthews, T.P., Poudel, J., Li, L., Wang, L.V., Anastasio, M.A.: Parameterized joint reconstruction of the initial pressure and sound speed distributions for photoacoustic computed tomography. SIAM Journal on Imaging Sciences **11**(2), 1560–1588 (2018)

[14] Liu, H., Uhlmann, G.: Determining both sound speed and internal source in thermo- and photo-acoustic tomography. Inverse Problems **31**(10), 105005 (2015)

[15] Yuan, Z., Zhang, Q., Jiang, H.: Simultaneous reconstruction of acoustic and optical properties of heterogeneous media by quantitative photoacoustic tomography. Optics Express **14**(15), 6749 (2006)

[16] Sun, Z., Sun, L.-S.: Simultaneous reconstruction of optical absorption property and speed of sound in intravascular photoacoustic tomography. Inverse Problems in Science and Engineering, 1–25 (2021)

[17] Groen, F.C.A., Young, I.T., Ligthart, G.: A comparison of different focus functions for use in autofocus algorithms. Cytometry **6**(2), 81–91 (1985)

[18] Krotkov, E.: Focusing. International Journal of Computer Vision **1**, 223–237 (1987)

[19] Minin, S.Y. P.: Sharpness estimation in facial images by spectrum approximation. SIViP **11**, 163–170 (2017)

[20] Treeby, B.E., Cox, B.T.: k-wave: Matlab toolbox for the simulation and reconstruction of photoacoustic wave fields. Journal of Biomedical Optics **15**(2), 021314 (2010)

[21] Isakov, V.: Inverse source problems. Mathematical Surveys and Monographs (1990)

[22] Otsu, N.: A threshold selection method from gray-level histograms. IEEE Transactions on Systems, Man, and Cybernetics **9**(1), 62–66 (1979)